



Change of the effective spin degeneracy in $\text{CeNi}_{9-x}\text{Cu}_x\text{Ge}_4$ due to the interplay between Kondo and crystal field effects

To cite this article: L. Peyker *et al* 2011 *EPL* **93** 37006

View the [article online](#) for updates and enhancements.

You may also like

- [Evolution of quantum criticality in \$\text{CeNi}_x\text{Cu}_{1-x}\text{Ge}_4\$](#)
L Peyker, C Gold, E-W Scheidt et al.
- [Local Spin Disorder in the Magnetic Kondo Compounds \$\text{CeNi}_x\text{Cu}_{1-x}\text{Ge}_4\$](#)
N Marcano, G M Kalvius, D R Noakes et al.
- [The development of specific heat and electrical resistivity in the \$\text{CeNi}_x\text{Pd}_{1-x}\text{In}\$ series](#)
M Klicpera, P Javorský and E Šantavá

Change of the effective spin degeneracy in $\text{CeNi}_{9-x}\text{Cu}_x\text{Ge}_4$ due to the interplay between Kondo and crystal field effects

L. PEYKER^{1(a)}, C. GOLD¹, W. SCHERER¹, H. MICHOR², T. UNRUH³, G. G. SIMEONI³, A. SENYSHYN^{3,4}, D. T. ADROJA⁵, O. STOCKERT⁶ and E.-W. SCHEIDT¹

¹ CPM, Institut für Physik, Universität Augsburg - 86159 Augsburg, Germany, EU

² Institut für Festkörperphysik, Technische Universität Wien - 1040 Wien, Austria, EU

³ Forschungsneutronenquelle Heinz Maier-Leibnitz, Technische Universität München - 85747 Garching, Germany, EU

⁴ Strukturforschung, Materialwissenschaft, Technische Universität Darmstadt - 64287 Darmstadt, Germany, EU

⁵ ISIS Facility, Rutherford Appleton Laboratory - Chilton, Didcot OX11 0QX, UK, EU

⁶ Max-Planck-Institut CPfS - 01187 Dresden, Germany, EU

received 23 June 2010; accepted in final form 19 January 2011

published online 15 February 2011

PACS 71.10.Hf – Non-Fermi-liquid ground states, electron phase diagrams and phase transitions in model systems

PACS 75.30.Mb – Valence fluctuation, Kondo lattice, and heavy-fermion phenomena

PACS 71.70.Ch – Crystal and ligand fields

Abstract – Elastic and inelastic neutron scattering experiments were carried out on the heavy-fermion systems $\text{CeNi}_{8.6}\text{Cu}_{0.4}\text{Ge}_4$ and $\text{CeNi}_8\text{CuGe}_4$ to study i) the influences of Ni/Cu substitution on the crystal field parameters and to identify ii) the driving forces of quantum criticality in $\text{CeNi}_{9-x}\text{Cu}_x\text{Ge}_4$. The relevance of competing RKKY and Kondo interactions and changes of the crystal field parameters is discussed. The crystallographic site where the Ni replacement by copper atoms takes place is identified by neutron powder diffraction studies. Furthermore, quasi-elastic and inelastic neutron scattering studies provide detailed information regarding the Kondo properties and the changes of the crystal field parameters resulting from the Ni/Cu replacement. Hence, a reduction of the effective spin degeneracy of the crystal field ground state with increasing Cu concentration is identified as one important control parameter of quantum criticality in $\text{CeNi}_{9-x}\text{Cu}_x\text{Ge}_4$. The results of these experiments are complemented by measurements of the thermopower.

Copyright © EPLA, 2011

Introduction. – Quantum criticality is a subject of intense debate in the physics of strongly correlated electrons because the presence of a quantum critical point (QCP) might be the prerequisite of non-Fermi liquid (NFL) behavior (for a recent review see [1,2]). It is manifested in the deviation of the temperature dependence of thermodynamic and transport properties from the usual Landau Fermi liquid behavior of metals, where a linear temperature dependence of the specific heat $C(T) = \gamma T$ is expected. The behavior of a system driven to a QCP is usually characterized by a divergence of the Sommerfeld coefficient $\gamma = C/T$ as the temperature approaches zero. In addition a competition between Kondo interactions favoring a paramagnetic Fermi liquid ground state and RKKY interactions preferring a magnetically ordered ground state is commonly observed in case of such a scenario (for recent reviews see [3,4]). Experimentally, the tuning of a system through a QCP can be accomplished

by i) applying pressure [5], ii) varying the sample composition stepwise [6], or iii) applying a magnetic field [7]. Apart from these classical QCP tuning mechanisms another control parameter was theoretically predicted by Coleman [8]: the *effective spin degeneracy* N . This parameter reflects the number of crystal field states separated by energies comparable or lower to the Kondo energy of the system. Its increase can prevent a system from magnetic ordering. In detail, the critical value of the Kondo coupling constant above which a spin-compensated ground state is stable tends to zero as $1/N$ with increasing N . Accordingly, a system with a large effective spin degeneracy N is less prone to exhibit a magnetically ordered ground state. In this context, CeNi_9Ge_4 is an interesting heavy-fermion system whose paramagnetic ground state might be stabilized by a quasi-fourfold effective spin degeneracy. It exhibits a very low T_K of a few Kelvin which is usually too small to inhibit long-range magnetic order in cerium Kondo lattice systems. Unique physical features of CeNi_9Ge_4 have been reported: beside single-ion

^(a)E-mail: ludwig.peyker@physik.uni-augsburg.de

NFL behavior in specific heat and magnetic susceptibility, the system exhibits a strongly enhanced value of the electronic specific heat $\Delta C/T \approx 5.5 \text{ Jmol}^{-1} \text{ K}^{-2}$ without showing any magnetic order [9,10]. This huge Sommerfeld coefficient could be mainly associated with Ce based single-ion effects, *i.e.*, crystal field and Kondo interactions, by studying the dilution series $\text{Ce}_{1-y}\text{La}_y\text{Ni}_9\text{Ge}_4$ [10]. In search of the origin of this behavior inelastic neutron scattering (INS) studies and single-crystal susceptibility analysis clarified the characteristics of the crystal field (CF) scheme and determined the Kondo energy of CeNi_9Ge_4 [11]. Due to the tetragonal symmetry of the system the ground state of Ce^{3+} with $j = \frac{5}{2}$ splits into three Kramer's doublets. Beside an excited doublet Γ_6 around 11 meV ($\cong 128 \text{ K}$) above the CF ground state, these studies surprisingly revealed a quasi-quartet ground state characterized by a subtle splitting into two doublets, $\Gamma_7^{(1)}$ and $\Gamma_7^{(2)}$. These doublets are separated by an energy of only $\Delta_1 \simeq 0.5 \text{ meV}$ ($\cong 6 \text{ K}$) which is in the range of the Kondo temperature $T_K \simeq 3.5 \text{ K}$. Accordingly, an enhanced effective spin degeneracy $N \simeq 4$ which is rather unusual for such NFL systems appears to be present in CeNi_9Ge_4 .

Based on these findings numerical renormalization group (NRG) calculations using the $SU(4)$ Anderson impurity model which also accounted for CF splitting demonstrated that the Kondo effect in combination with a quasi-quartet ground state leads to a $SU(2)$ -to- $SU(4)$ crossover regime with a significant variation of the Sommerfeld-Wilson ratio as experimentally observed in $\text{Ce}_{1-y}\text{La}_y\text{Ni}_9\text{Ge}_4$ [12,13].

In contrast, a gradual replacement of Ni by Cu in CeNi_9Ge_4 leads to the formation of long-range antiferromagnetic order in $\text{CeNi}_8\text{CuGe}_4$ with $T_N = 175 \text{ mK}$ [14]. Profound analysis of the specific heat, thermal expansion, magnetic susceptibility, electrical resistivity and preliminary INS studies of the substitution series $\text{CeNi}_{9-x}\text{Cu}_x\text{Ge}_4$ reveals that the electronic nature of this system can be continuously tuned from an effectively fourfold degenerate nonmagnetic Kondo ground state in CeNi_9Ge_4 towards a magnetically ordered, effectively twofold degenerate ground state in $\text{CeNi}_8\text{CuGe}_4$ [14,15]. At a suitable Cu concentration of $x \simeq 0.4$, where a crossover between single-ion and magnetic ordered behavior occurs, the system exhibits quantum critical behavior with χ and $C/T \propto -\ln T$ [16] and an enhanced Grüneisen parameter [14]. In contrast to the common quantum critical scenario, where the transition is driven by the competition between Kondo effect and RKKY interaction, we proposed that in this system the reduction of the effective CF ground-state degeneracy plays a relevant role in provoking long-range magnetic order [14].

With this letter we present a study on the microscopic Kondo and CF energy scales which depend on the Ni/Cu substitution. Therefore, neutron scattering experiments on the compounds $\text{CeNi}_{8.6}\text{Cu}_{0.4}\text{Ge}_4$ and $\text{CeNi}_8\text{CuGe}_4$ were performed at the research reactor FRM-II (Garching, Germany). These studies helped to clarify the structural changes upon Ni substitutions and to determine their

influence on the CF level scheme. The inelastic neutron scattering studies were carried out on the time-of-flight spectrometer TOFTOF [17], while the elastic scattering studies were performed at the high-resolution structure powder diffractometer SPODI ($\lambda = 1.5483 \text{ \AA}$) [18]. Complementary elastic neutron scattering studies were performed on $\text{Ce}^{60}\text{Ni}_9\text{Ge}_4$ at the High Resolution Powder Diffractometer (HRPD) instrument at ISIS Facility (Oxfordshire, United Kingdom).

Sample preparation and structural characterization. – The polycrystalline samples of $\text{CeNi}_{8.6}\text{Cu}_{0.4}\text{Ge}_4$, $\text{CeNi}_8\text{CuGe}_4$ and of the nonparamagnetic reference compounds $\text{LaNi}_{8.6}\text{Cu}_{0.4}\text{Ge}_4$, $\text{LaNi}_8\text{CuGe}_4$ were synthesized by arc melting the pure elements Ce: 4N; La: 3N8 (Ames MPC [19]); Ni: 4N5; Cu: 6N; Ge: 5N, under a highly purified argon atmosphere. Subsequently the samples were annealed in evacuated quartz tubes for one week at 950°C . Additionally a $\text{Ce}^{60}\text{Ni}_9\text{Ge}_4$ sample with ^{60}Ni enriched Ni metal (STB Isotope Germany GmbH: 10.7% ^{58}Ni , 89.0% ^{60}Ni , 0.3% ^{61}Ni ; 3N chemical purity) was synthesized by induction melting. X-ray diffraction experiments showed that all samples are single-phase materials. They crystallize in the LaFe_9Si_4 -type structure (tetragonal space group $I4/mcm$) with three Ni sites (Ni1:16k, Ni2:16l, Ni3:4d), one Ge (16l) and one Ce site (4a). Due to the minor differences in the scattering factors of Ni and Cu these experiments could not reveal any ordering of copper in the lattice.

Elastic neutron scattering. – In order to further scrutinize the structural model assuming an ordered occupation of Ni and Ge sites, a $\text{Ce}^{60}\text{Ni}_9\text{Ge}_4$ neutron powder diffraction study was performed at 250 K with a sample (6 g) placed in a cylindrical vanadium can. The difference between the averaged neutron scattering length of 89.0% isotope enriched ^{60}Ni (4.06 fm) and that of Ge (8.185 fm) clearly increases compared to the one derived from the natural abundance of Ni isotopes (10.3 fm). Crystallographic analysis was performed by the Rietveld method whereby the best fit is obtained by a structural model assuming a fully ordered arrangement of Ce, Ni, and Ge atoms in the space group $I4/mcm$ (see table 1).

For the purpose of studying the influences of the Ni/Cu substitution on the CF, it was essential to investigate, which of the individual Ni sites is preferentially occupied by Cu, and to estimate the degree of Ni/Cu disorder in $\text{CeNi}_8\text{CuGe}_4$. Therefore a neutron diffraction experiment was performed at 300 K and 4 K, where the compound was filled in a single-walled cylindrical vanadium container (14 mm in diameter, 0.15 mm wall thickness). First, the sample homogeneity was checked by a full profile decomposition technique, where the background (determined by a linear interpolation between points in non-overlapping regions), lattice, profile (Pseudo-Voigt function) and asymmetry parameters were refined. A rather weak, but still noticeable reflection broadening was observed over the entire Q -range accessible in the diffraction experiment. After deconvolution with the

Table 1: (Color online) Structural parameters of $\text{Ce}^{60}\text{Ni}_9\text{Ge}_4$ and $\text{CeNi}_8\text{CuGe}_4$ obtained from refinements of neutron powder diffraction data by a full profile Rietveld analysis. The space group is $I4/mcm$ (No. 140). The figure on the right shows the Ce coordination. The Ge/Ni sites are indicated via dashed/solid connection lines, respectively. The substitution of nickel by 25% copper atoms on the 16k sites is schematically highlighted, salient interatomic distances are specified in pm.

$\text{Ce}^{60}\text{Ni}_9\text{Ge}_4$ at $T = 250$ K				
Lattice parameters $a = 7.9562(3)$ Å, $c = 11.7525(5)$ Å				
Atom sites	x/a	y/b	z/c	u_{iso} (Å ²)
Ce, 4a, 422	0	0	0.25	0.0089(3)
Ge, 16l, ..m	0.17333(3)	0.67333(3)	0.12249(2)	0.0066(2)
Ni, 4d, m.mm	0.0	0.5	0.0	0.0083(4)
Ni, 16k, m..	0.06721(8)	0.20286(8)	0	0.0030(3)
Ni, 16l, ..m	0.62429(8)	0.12429(8)	0.18095(6)	0.0086(3)

$$R_p : 4.38\%; R_{wp} : 4.01\%; R_{exp} : 1.79\%; \chi^2 : 5.01$$

$\text{CeNi}_8\text{CuGe}_4$ at $T = 4$ K				
Lattice parameters $a = 7.95941(9)$ Å, $c = 11.79895(16)$ Å				
Atom sites	x/a	y/b	z/c	u_{iso} (Å ²)
Ce, 4a, 422	0	0	0.25	0.0016(8)
Ge, 16l, ..m	0.17271(11)	0.67271(11)	0.12369(9)	0.0081(3)
Ni, 4d, m.mm	0	0.5	0	0.0062(4)
Ni/Cu*, 16k, m..	0.06782(12)	0.20365(13)	0	0.0058(2)
Ni, 16l, ..m	0.62437(9)	0.12437(9)	0.18080(7)	0.00567(19)

$$R_p : 2.31\%; R_{wp} : 3.11\%; R_{exp} : 1.21\%; \chi^2 : 6.68$$

*Site with mixed occupancy: 75 at. % Ni, 25 at. % Cu

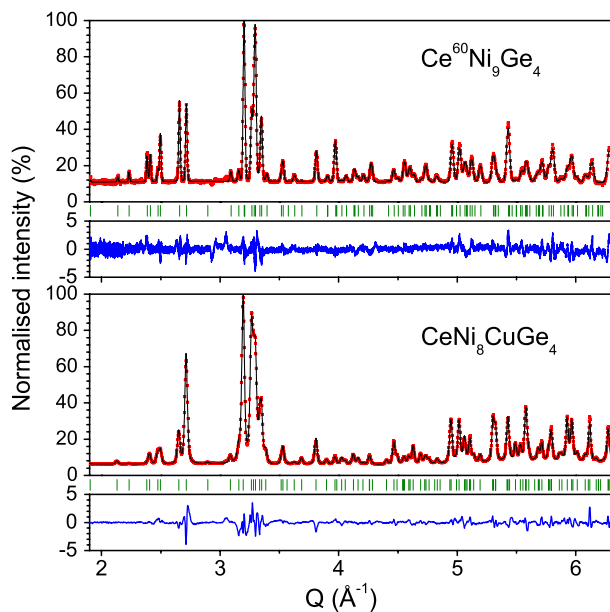
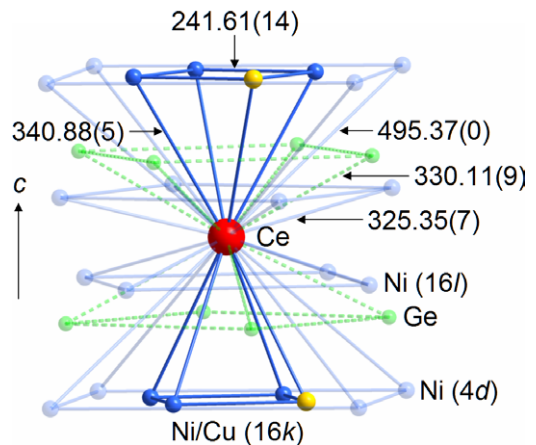


Fig. 1: (Color online) Results of Rietveld refinement for neutron powder diffraction data for $\text{Ce}^{60}\text{Ni}_9\text{Ge}_4$ at 250 K (HRPD) and for $\text{CeNi}_8\text{CuGe}_4$ at 4 K (SPODI). Experimental data are shown by points, the continuous line denotes the calculated profile and the lower plot represents the difference between the observed and calculated intensity. Calculated positions of Bragg reflections are shown by vertical tick marks.

instrumental resolution function this line broadening could be assigned to a size-effect, which was best simulated with platelet-like shaped crystallites (ca. 400 Å in diameter and surfaces aligned parallel to [200]). In further structure considerations, based on the Rietveld method,

these observed weak microstructural effects were included by simultaneous refinements of the Caglioti profile parameters. To localize the copper atoms in the lattice, all copper atoms were statistically distributed over three Ni sites at the initial stage of our model development. During the progress of our Rietveld refinement the dominant occupation of copper on the Ni site with 16k symmetry (99 at.% after convergence, fig.1) became more and more obvious. In the final step, the occupancy of this mixed Ni/Cu site (75%/25%) and of the Ce site (100%) was kept fixed. This refinement yields a little excess of the occupancy on the 16l-sites of both Ni (101.2(4)%) and Ge (101.0(6)%). This result is probably related to a weak static disorder existing in the material. The preferred occupation of the 16k sites by the copper atoms is in line with band structure calculations based on the full-potential augmented spherical wave method [14]. These clearly support an energetic preference for a Ni/Cu substitution at the 16k site with $m..$ point symmetry. According to that and due to the stoichiometric substitution, it can be assumed that on average every fourth atom on this 16k site is statistically replaced by copper. We note that this replacement does not lead to any noticeable superstructural reflections, hence the local site symmetry of Ce can still be approximated by 422.

Inelastic neutron scattering. – While the CF parameters of $\text{CeNi}_8\text{CuGe}_4$ were identified by a detailed analysis of the INS data published in [15] additional neutron scattering experiments were carried out to determine the CF parameters of $\text{CeNi}_{8.6}\text{Cu}_{0.4}\text{Ge}_4$. The studies were accomplished with about 35 g of $\text{CeNi}_{8.6}\text{Cu}_{0.4}\text{Ge}_4$

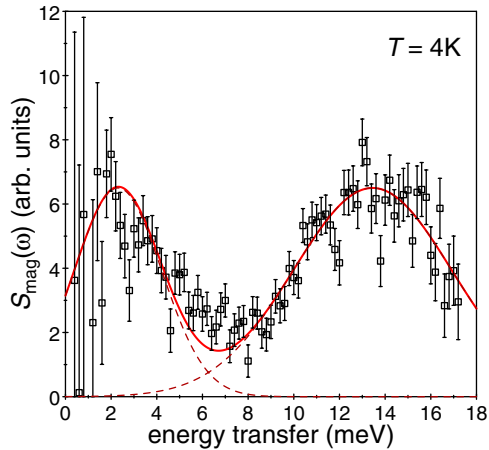


Fig. 2: (Color online) Magnetic scattering function $S_{\text{mag}}(\omega)$ of $\text{CeNi}_{8.6}\text{Cu}_{0.4}\text{Ge}_4$ at 4 K. The solid line represents a fit to a spectral function consisting of two Gaussians (dashed line).

filled in a thin double-walled aluminium can which was mounted onto a closed-cycle refrigerator. To determine the phonon part of the scattering and the detector efficiency, additionally, the nonparamagnetic reference compound $\text{LaNi}_{8.6}\text{Cu}_{0.4}\text{Ge}_4$ and a vanadium standard have been measured. The INS experiments were performed at a sample-temperature of 4 K with an incident neutron energy of $E_i = 20.5$ meV. A modified version of the program IDA written by Wuttke [20] was used to carry out the data analysis. The main challenge in the quantitative interpretation of measured INS spectra is to derive the phonon contribution correctly, particularly in compounds, such as $\text{CeNi}_{8.6}\text{Cu}_{0.4}\text{Ge}_4$ containing elements with large nuclear cross sections. For the extraction of the magnetic signal from the large phononic background the different Q -dependences were used as described in [21]. First, the nonparamagnetic reference compound was used to determine the ratio of the high-angle and low-angle scattering intensities. Then this ratio was used to scale the high- Q to the low- Q response in $\text{CeNi}_{8.6}\text{Cu}_{0.4}\text{Ge}_4$ and to subtract the phonon contribution (for details see [15]). In the final step the quasi-elastic scattering, which arises due to the Kondo effect (see below), was subtracted by a single Lorentzian combined with a Bose distribution to determine the magnetic excitations also at low energies. The corrected data, which show the magnetic scattering contribution $S_{\text{mag}}(\omega)$ of $\text{CeNi}_{8.6}\text{Cu}_{0.4}\text{Ge}_4$, are displayed in fig. 2. In the spectrum around 2 meV and 13.5 meV two broad excitations are observed and assigned to magnetic transitions. Each excitation was fitted with a Gaussian-function (dashed line). The final fit (solid line) provides the values of the CF splitting energies: $\Delta_1 \approx 2.3 \pm 0.2$ meV (≈ 27 K) and $\Delta_2 \approx 13.5 \pm 0.2$ meV (≈ 157 K). On the basis of a simple CF approach the sixfold degenerate CF ground state ($J = \frac{5}{2}$) of Ce^{3+} ions displaying a tetragonal symmetry will split in the presence of the crystal field into three doublets separated by the respective energies Δ_1 and Δ_2 above the CF

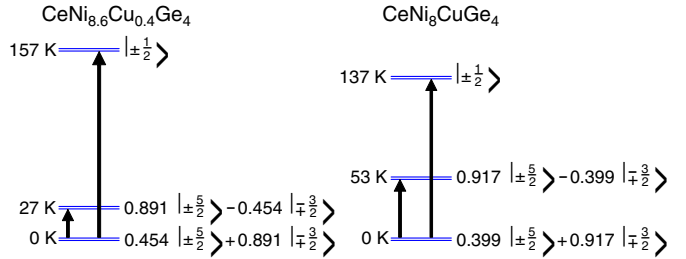


Fig. 3: (Color online) The CF level scheme and f -electron wave functions of Ce^{3+} in $\text{CeNi}_{8.6}\text{Cu}_{0.4}\text{Ge}_4$ and $\text{CeNi}_8\text{CuGe}_4$.

ground-state level. The CF Hamiltonian for this case can be written as

$$H_{\text{CF}} = B_2^0 O_2^0 + B_4^0 O_4^0 + B_4^4 O_4^4, \quad (1)$$

where B_l^m and O_l^m represent the phenomenological CF parameters and the Stevens operator equivalents, respectively. A detailed analysis of the CF results in a couple of CF parameter sets which reproduce the energy levels. Considering also the intensity ratio of the two CF excitations, the best CF parameter set, which conforms to the data is $B_2^0 = -6.30$ K, $B_4^0 = 0.38$ K and $B_4^4 = -0.40$ K.

As basis for the determination of the CF parameters of $\text{CeNi}_8\text{CuGe}_4$ the CF scheme identified in [15] was used. With the same CF approach used above, the CF excitations of $\text{CeNi}_8\text{CuGe}_4$ at 4.6 meV (≈ 53 K) and 11.8 meV (≈ 137 K) lead to the following CF parameter set: $B_2^0 = -4.00$ K, $B_4^0 = 0.35$ K and $B_4^4 = -0.72$ K. Accordingly, the CF parameter which exhibits the most significant change is B_2^0 , where the value increases from -6.3 K to -4.0 K. The diagonalization of the CF Hamiltonian yields the wave functions displayed in fig. 3, where also the resulting CF level schemes with its three Kramer's doublets are shown.

To study the dynamic behavior of the stable $4f$ -moments coupled to the conduction electrons, the quasi-elastic scattering was analyzed at different temperatures. An incident neutron energy of $E_i = 2.3$ meV has been chosen. In order to obtain the magnetic scattering of the cerium the nonmagnetic La reference data representing phonon plus background contribution was simply subtracted from the Ce data, because the coherent and incoherent cross section of both materials match each other within a few percent. After that the data was integrated over the whole Q -range. The resulting magnetic correlation functions $S_{\text{mag}}(\omega)$ are plotted in fig. 4. To describe these experimental results a relaxation ansatz for the scattering law consisting of a single Lorentzian combined with a Bose distribution was made as suggested in [22]:

$$\begin{aligned} S(\omega, T) &= \frac{1}{1 - \exp(-\beta\omega)} \text{Im} \chi(\omega, T) \\ &= \frac{1}{1 - \exp(-\beta\omega)} \chi_0(T) \omega \frac{\Gamma(T)}{\omega^2 + \Gamma(T)^2}, \quad (2) \end{aligned}$$

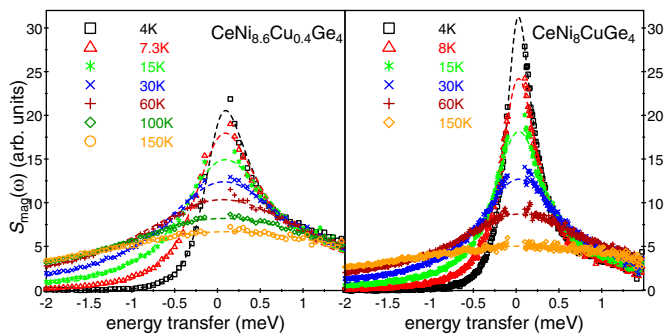


Fig. 4: (Color online) Quasi-elastic scattering functions $S_{\text{mag}}(\omega)$ of $\text{CeNi}_{8.6}\text{Cu}_{0.4}\text{Ge}_4$ and $\text{CeNi}_8\text{CuGe}_4$ at different temperatures as labeled. The dashed lines represent a fit based on eq. (2).

where $\Gamma(T)$ and $\chi_0(T)$ are the temperature-dependent quasi-elastic line width (relaxation rate) and the static susceptibility, respectively, and $\beta = 1/k_B T$. The experimental results are in a very good agreement with the relaxation ansatz (see fig. 4). Additionally, the estimated trend of the static susceptibility $\chi_0(T)$ values gained from the fit match very well the susceptibility results published in [14]. Figure 5 shows a comparison between neutron and magnetometer data. The insert in fig. 5 displays the temperature dependence of the line width $\Gamma(T)$ obtained from the fit according to eq. (2). Neither a Korringa-type behavior, as predicted by the theory of Becker *et al.* (BFK) [23], nor a \sqrt{T} dependence as observed in [24] describes the temperature dependence of the quasi-elastic line width $\Gamma(T)$ and thus the relaxation behavior of the low-frequency part of the dynamic susceptibility. The discrepancy to the BFK theory, which accounts for stable magnetic moments, is due to the presence of the Kondo effect, which is intrinsic to the system $\text{CeNi}_{9-x}\text{Cu}_x\text{Ge}_4$ [14] and causes a strong screening of the moments of the Ce^{3+} ions at low temperatures [16]. Consequently, the line width of the quasi-elastic line remains finite as $T \rightarrow 0$. An extrapolation of $\Gamma(T)$ yields a finite value of $\Gamma(0) \approx 2.7\text{K}$ for $\text{CeNi}_{8.6}\text{Cu}_{0.4}\text{Ge}_4$ and $\Gamma(0) \approx 1.3\text{K}$ for $\text{CeNi}_8\text{CuGe}_4$ for $T \rightarrow 0$ which is in line with the Kondo temperature T_K assumed for model calculations of the specific heat in [14]. This low-temperature Kondo energy scale could be the reason for disagreement with the \sqrt{T} behavior. Nevertheless a power law $\Gamma(T) = \Gamma_0 + cT^b$ with an exponent $b \approx 0.8$ shows good agreement with the experimental data.

Thermopower. – The thermopower was measured in a commercial PPMS with a thermal transport option. In fig. 6 the Seebeck coefficient S of $\text{CeNi}_{9-x}\text{Cu}_x\text{Ge}_4$ for $x = 0; 0.4; 1$ is shown. For CeNi_9Ge_4 two broad maxima can be observed. The upper maximum gives a hint for the overall splitting of the CF [25]. Furthermore, the lower one can be associated with the interaction between the Kondo effect and a small CF splitting involving ground state and first

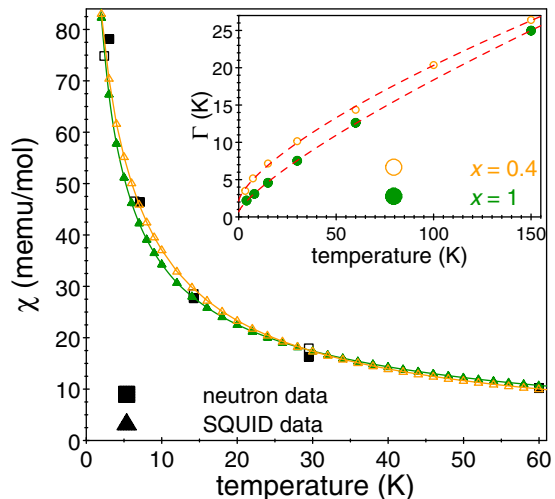


Fig. 5: (Color online) Static susceptibility $\chi_0(T)$ of neutron and SQUID magnetometer measurements. $\text{CeNi}_{8.6}\text{Cu}_{0.4}\text{Ge}_4$ is represented by open, $\text{CeNi}_8\text{CuGe}_4$ by solid symbols. The neutron values are normalized at 60 K to the dc susceptibility data. The insert shows the temperature dependence of the line width $\Gamma(T)$ obtained with eq. (2). The dashed lines represent a power law fit.

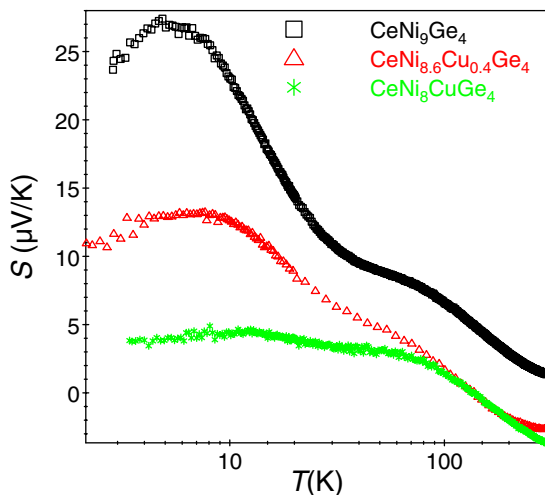


Fig. 6: (Color online) Seebeck coefficient of $\text{CeNi}_{9-x}\text{Cu}_x\text{Ge}_4$ for $x = 0; 0.4; 1$.

excited Kramer's doublet ($\Delta_1 \approx T_K$). This reflects an effective degeneracy of $N = 4$. By Ni/Cu substitution in this compound, the position of the upper maximum, connected to the overall CF splitting, remains almost the same. In contrast, the lower maximum shifts to higher temperatures and broadens with increasing x . These changes are based on a reduction of the Kondo temperature and the increase of the interlevel splittings between the two low-lying Kramer's doublets. This again is a clear hint for a reduction of the effective degeneracy. Additionally, the decrease of the effective degeneracy is reflected by a reduction of the thermopower values, like it was found for $\text{Ce}_{1-x}\text{La}_x\text{TiGe}$ [26]. The fact, that the low-temperature thermopower values decreases more significantly for $x = 1$

than for $x = 0.4$ is due to the emergence of antiferromagnetic fluctuations in $\text{CeNi}_8\text{CuGe}_4$.

Conclusions. – We have shown that upon Ni/Cu substitution Cu replaces the atoms at the Ni1 ($16k$) sites. Accordingly, the symmetry of the Ce site can still be approximated by a 422 point symmetry. The fourfold degenerate ground state of CeNi_9Ge_4 splits due to the modified CF in a twofold degenerate Kondo ground state $\Gamma_7^{(2)}$ ($T_K = 2.7\text{K}$ for $x = 0.4$ and $T_K = 1.3\text{K}$ for $x = 1$, determined by the quasi-elastic scattering) and an excited doublet $\Gamma_7^{(1)}$ ($\Delta_1 \approx 27\text{K}$ for $x = 0.4$ and $\Delta_1 \approx 53\text{K}$ for $x = 1$) which could be observed in the INS spectra. The energy splitting Δ_2 between the second excited doublet Γ_6 and the CF ground state $\Gamma_7^{(2)}$, however, remains almost in the same range. Hence, Ni/Cu substitution in $\text{CeNi}_8\text{CuGe}_4$ causes a splitting of the quasi-quartet ground state. So the effective degeneracy of the CF ground state reduces with increasing Cu content due to the additional anisotropy along the c -axis induced by the Ni/Cu substitution. This is supported by the strong change of the CF parameter B_2^0 , which usually defines the magnetic anisotropy [27].

By means of INS and thermopower experiments it could be verified, that the effective spin degeneracy N can be continuously tuned by substitution. In the parent compound CeNi_9Ge_4 the fourfold effective spin degeneracy suppresses magnetic order, despite the occurrence of strong antiferromagnetic correlations. The continuous decrease of N in combination with a reduction of the Kondo temperature in the substitution series $\text{CeNi}_{9-x}\text{Cu}_x\text{Ge}_4$, drives the system to long-range antiferromagnetic order which provokes a QCP scenario. A similar magnetic phase diagram was found when Ni is replaced by Co [28]. Hereby a distinct increase of the Kondo temperature is observed. But counter-intuitive to the Doniach picture antiferromagnetic order appears. This again results from the reduction of the effective spin degeneracy due to an increase of the CF splitting. Apparently the change of the effective spin degeneracy provides a new tuning mechanism towards a quantum phase transition in heavy-fermion systems.

We would like to thank A. DAOUD-ALADINE for performing diffraction experiment on HRPD at ISIS Facility. This work was supported by the Deutsche Forschungsgemeinschaft (DFG) under Contract No. SCHE487/7-1/2.

REFERENCES

- [1] STEWART G. R., *Rev. Mod. Phys.*, **73** (2001) 797.
- [2] STEWART G. R., *Rev. Mod. Phys.*, **78** (2006) 743.
- [3] v. LÖHNEYSEN H., ROSCH A., VOJTA M. and WÖLFLE P., *Rev. Mod. Phys.*, **79** (2007) 1015.
- [4] GEGENWART P., SI Q. and STEGLICH F., *Nat. Phys.*, **4** (2008) 186.
- [5] BOGENBERGER B. and v. LÖHNEYSEN H., *Phys. Rev. Lett.*, **74** (1995) 1016.
- [6] ANDRAKA B. and STEWART G. R., *Phys. Rev. B*, **47** (1993) 3208.
- [7] HEUSER K., SCHEIDT E.-W., SCHREINER T. and STEWART G. R., *Phys. Rev. B*, **57** (1998) 4198.
- [8] COLEMAN P., *Phys. Rev. B*, **28** (1983) 5255.
- [9] MICHOR H., BAUER E., DUSEK C., HILSCHER G., ROGL P., CHEVALIER B., ETOURNEAU J., GIESTER G., KILLER U. and SCHEIDT E.-W., *J. Magn. & Magn. Mater.*, **272** (2004) 227.
- [10] KILLER U., SCHEIDT E.-W., EICKERLING G., MICHOR H., SERENI J., PRUSCHKE T. and KEHREIN S., *Phys. Rev. Lett.*, **93** (2004) 216404.
- [11] MICHOR H., ADROJA D. T., BAUER E., BEWLEY R., DOBOZANOV D., HILLIER A. D., HILSCHER G., KILLER U., KOZA M., MANALO S., MANUEL P., REISSNER M., ROGL P., ROTTER M. and SCHEIDT E.-W., *Physica B*, **378** (2006) 640.
- [12] SCHEIDT E.-W., MAYR F., KILLER U., SCHERER W., MICHOR H., BAUER E., KEHREIN S., PRUSCHKE T. and ANDERS F., *Physica B*, **378** (2006) 154.
- [13] ANDERS F. B. and PRUSCHKE T., *Phys. Rev. Lett.*, **96** (2006) 86404.
- [14] PEYKER L., GOLD C., SCHEIDT E.-W., SCHERER W., DONATH J. G., GEGENWART P., MAYR F., UNRUH T., EYERT V., BAUER E. and MICHOR H., *J. Phys.: Condens. Matter*, **21** (2009) 235604.
- [15] PEYKER L., GOLD C., SCHEIDT E.-W., MICHOR H., UNRUH T., SENYSHYN A., STOCKERT O. and SCHERER W., *J. Phys.: Conf. Ser.*, **200** (2010) 012160.
- [16] PEYKER L., GOLD C., SCHEIDT E.-W., MICHOR H. and SCHERER W., *J. Phys.: Conf. Ser.*, **200** (2010) 012176.
- [17] UNRUH T., MEYER A., NEUHAUS J. and PETRY W., *Neutron News*, **18** (2007) 22.
- [18] HOELZEL M., SENYSHYN A., GILLES R., BOYSEN H. and FUESS H., *Neutron News*, **18** (2007) 23.
- [19] Material Preparation Center, Ames Laboratory, US DOE Basic Energy Sciences, Ames, IA, USA available from: www.mpc.ameslab.gov.
- [20] See <http://sourceforge.net/projects/frida/>.
- [21] MURANI A. P., *Phys. Rev. B*, **50** (1994) 9882.
- [22] FULDE P. and LOEWENHAUPT M., *Adv. Phys.*, **34** (1985) 589.
- [23] BECKER K. W., FULDE P. and KELLER J., *Z. Phys. B: Condens. Matter*, **28** (1977) 9.
- [24] HORN S., STEGLICH F., LOEWENHAUPT M. and HOLLAND-MORITZ E., *Physica B + C*, **107** (1981) 103.
- [25] ZLATIĆ V. and MONNIER R., *Phys. Rev. B*, **71** (2005) 165109.
- [26] OESCHLER N., DEPPE M., HARTMANN S., CAROCA-CANALES N., GEIBEL C. and STEGLICH F., *J. Phys.: Conf. Ser.*, **200** (2010) 012148.
- [27] GOREMYCHKIN E. A., MUZYCHKA A. YU. and OSBORN R., *Physica B*, **179** (1992) 184.
- [28] PEYKER L., GOLD C., SCHERER W., MICHOR H. and SCHEIDT E.-W., arXiv:1011.5143v1, to be published in *J. Phys.: Conf. Ser.*